

SAND98-0681A  
SAND-98-0681C

End-face preparation methods for high-intensity fiber applications

Robert E. Setchell

CONF-9710116--

RECEIVED

MAR 20 1998

OSTI

Sandia National Laboratories, MS1421  
Albuquerque, New Mexico 87185

ABSTRACT

High laser intensities are being transmitted through optical fibers in a growing number of applications. Our interest in laser initiation of explosives has led us to examine the transmission of Q-switched, Nd:YAG laser pulses through step-index, multimode, fused-silica fibers for a number of years. A common limiting process is a plasma-forming breakdown occurring at the fiber entrance face. The breakdown threshold at this face depends on the surface characteristics that result from the particular method of end-face preparation. In previous studies we examined entrance-face breakdown thresholds for several different mechanical polishing schedules, and also for several schedules of CO<sub>2</sub>-laser conditioning following mechanical polishing. In the present study we examined three end-face preparation methods that were based on the recent availability of exceptionally good cleaved surfaces for our fibers of interest. Using test procedures similar to those in past studies, we examined the cleaved fibers directly, fibers with cleaved surfaces that were subsequently flame polished, and fibers with cleaved surfaces that were subsequently conditioned with a CO<sub>2</sub> laser. All of these preparation methods resulted in fibers that showed a broader range of entrance-face breakdown conditions than found in past studies, together with a susceptibility to subsurface exit-face damage. By introducing additional cleaning steps with the cleaved surfaces, we were able to reduce the variability in breakdown thresholds observed after subsequent CO<sub>2</sub>-laser conditioning. A consistent location of exit-face damage sites indicates that subsurface fracturing occurs during the cleaving process, and that the subsequent end-face processing steps were not effective in mitigating damage at these sites.

Threshold energies for entrance-face breakdown are also affected by the relation between incident laser energy and the resulting peak local fluence at this surface. Laser characteristics and the design of the laser-to-fiber injection optics determine this relation. The present study utilized an improved injection system consisting of a custom diffractive optical element combined with a lens having a very short focal length. This system produced the lowest value for the ratio of peak-to-average fluence at the entrance face that we have observed, and was very successful in inhibiting internal damage mechanisms along the fiber path.

**Keywords:** fiber optics, fiber damage, cleaved fibers, flame polishing, CO<sub>2</sub>-laser conditioning, diffractive optics

1. INTRODUCTION

A recent review<sup>1</sup> addressed the growing number of applications involving high-intensity laser transmission through optical fibers. Our particular interest is the use of fibers during laser initiation of explosives, and our corresponding studies have examined the transmission of Q-switched, Nd:YAG laser pulses through step-index, multimode, fused-silica fiber.<sup>2-7</sup> A number of breakdown and damage processes have been observed, as indicated in Fig. 1. System factors that can affect the threshold conditions for these limiting processes have been identified.<sup>7</sup> A common limiting process is a plasma-forming breakdown at the fiber entrance face, and in several previous studies we examined the role of fiber end-face preparation methods and corresponding surface characteristics in determining breakdown thresholds. These preparation methods included different mechanical polishing schedules,<sup>2,3</sup> adding CO<sub>2</sub>-laser conditioning following mechanical polishing,<sup>3,4,7</sup> and cleaving.<sup>5,7</sup> The highest thresholds observed in these studies corresponded to specific CO<sub>2</sub>-laser conditioning schedules added to mechanically polished end faces. Unfortunately, this is the preparation method requiring the most specialized equipment as well as human skill and time, and consequently the most expensive for high-volume applications. Cleaved surfaces are intuitively appealing in terms of their apparent preparation simplicity and their freedom from polishing contaminants. In practice, however, obtaining a mirror-like cleaved surface free from areas of surface roughness ("mist" and "hackle" zones) is quite difficult for fiber diameters as large as we have used (up to 440 microns). Measured thresholds were discouraging in one previous study using cleaved surfaces supplied by a commercial vendor.<sup>5</sup> This lot of test fibers had very smooth end faces, but many of the faces appeared to have small specks of contamination that we could not remove,

19980420 061

DISTRIBUTION OF THIS DOCUMENT IS UNLIMITED



MASTER

### **DISCLAIMER**

This report was prepared as an account of work sponsored by an agency of the United States Government. Neither the United States Government nor any agency thereof, nor any of their employees, makes any warranty, express or implied, or assumes any legal liability or responsibility for the accuracy, completeness, or usefulness of any information, apparatus, product, or process disclosed, or represents that its use would not infringe privately owned rights. Reference herein to any specific commercial product, process, or service by trade name, trademark, manufacturer, or otherwise does not necessarily constitute or imply its endorsement, recommendation, or favoring by the United States Government or any agency thereof. The views and opinions of authors expressed herein do not necessarily state or reflect those of the United States Government or any agency thereof.

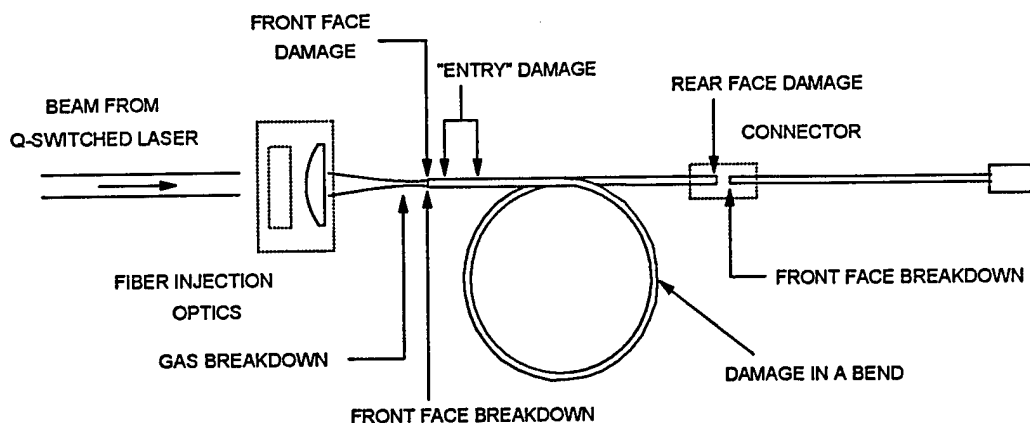


Fig. 1 Breakdown and damage processes in a high-intensity fiber transmission system

and the lot showed a particular susceptibility to exit-face damage. In contrast, limited front-surface testing of some very large fibers cleaved by a different commercial vendor<sup>8</sup> indicated that these surfaces were very resistant to entrance-face breakdown.<sup>7</sup> This led us to obtain a large number of cleaved fiber samples from this vendor for use in the current study. The vendor had also implemented flame polishing of end faces as a means of eliminating the sharp edges typical of a cleaved surface. Early work on damage thresholds for bare surfaces had identified flame polishing as a means for significantly raising thresholds.<sup>9</sup> Consequently, we obtained a number of fiber samples from the same vendor that were flame polished following cleaving. Finally, using cleaved samples from this vendor, we developed a schedule for CO<sub>2</sub>-laser conditioning of the cleaved surfaces for comparison with previous results on similarly conditioned end faces that had been mechanically polished.

In addition to surface characteristics, energy thresholds for entrance-face breakdown are affected by the relation between incident laser energy and the resulting peak local fluence at this surface. This relation is determined by laser characteristics and the design of the laser-to-fiber injection optics. By the use of magnified beam-profiling techniques, the actual fluence distribution on a fiber entrance face resulting from a particular combination of laser and injection optics can be established. A figure of merit for laser conditions at the entrance face can be defined by the following ratio of peak-to-average fluences:

$$P / A = \frac{\text{peak local fluence}}{(\text{total energy incident on fiber core}) / (\text{fiber core area})}$$

In practice, the incident laser energy is confined to the fiber core to prevent energy from propagating in the cladding. A perfect "flat top" fluence distribution extending over the entire core area would achieve a value of unity for this ratio. Using different lasers and injection optics, we have achieved values for this ratio varying from less than 3 to more than 5. The highest values have resulted from simple lens injection of multimode laser beams having very strong "hot spots".

The injection optics can also influence internal damage thresholds within the initial "entry" segment and at the first bend in the fiber path.<sup>7</sup> Desirable attributes for inhibiting these damage mechanisms include some means of preventing internal focusing of the beam immediately beyond the entrance face, and some means of generating a broad mode power distribution in the fiber as early as possible along its path. Prevention of internal focusing is difficult using conventional optics, but the generation of a broad mode power distribution was achieved in an earlier study using a mechanical mode scrambler.<sup>7</sup> In the present study, both of these attributes were achieved using a custom diffractive optical element combined with a lens having a very short focal length. This injection system also achieved the lowest ratio of peak-to-average fluences that we have observed at a fiber entrance face.

The next section summarizes the experimental procedures for routine damage testing of optical fibers. The following section provides details on the design and performance of the new injection optics. Subsequent sections present and discuss the threshold data obtained with these optics on fibers having end faces that are cleaved, cleaved plus flame polished, and cleaved plus CO<sub>2</sub>-laser conditioned.

## 2. PROCEDURES FOR FIBER DAMAGE TESTING

The basic experimental configuration used for obtaining breakdown and damage statistics on optical fibers is shown schematically in Fig. 2. The test laser is a compact, oscillator-only, multimode Nd:YAG (Laser Photonics Model YQL-102)

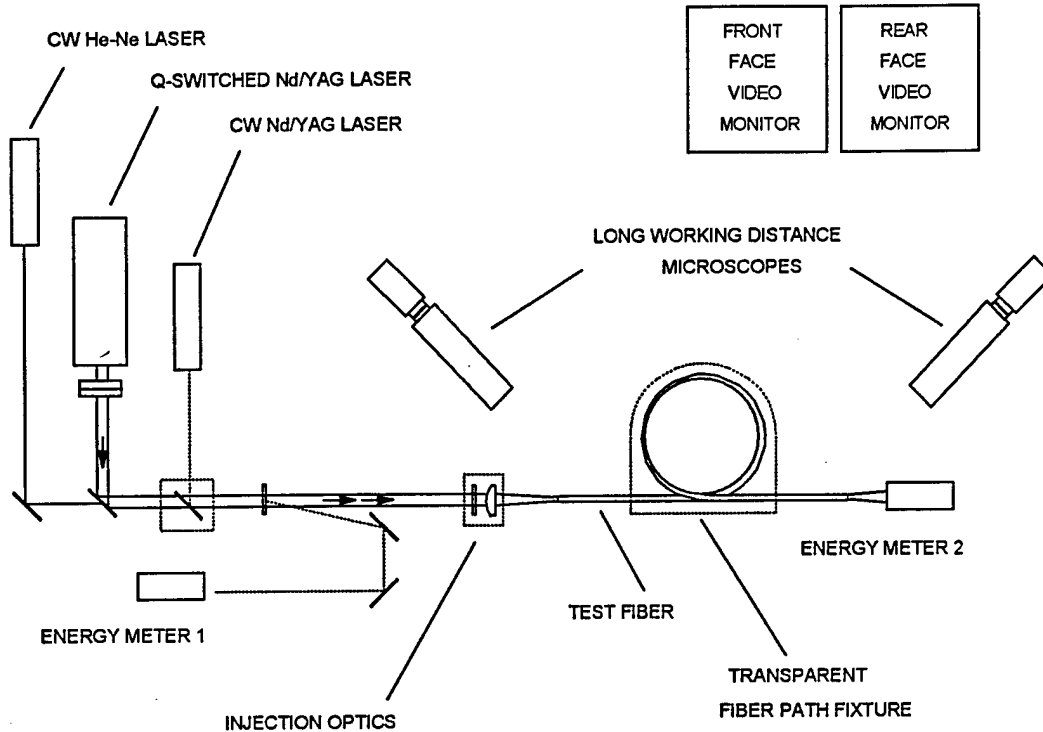


Fig. 2 Experimental configuration for fiber damage testing

operated at the fundamental wavelength ( $1.064 \mu\text{m}$ ) in a Q-switched, single-shot mode. This laser had been modified previously to produce nearly Gaussian near-field and far-field profiles while preserving its full multimode output energy. Because of higher losses in the injection optics (described in the next section), the flashlamp voltage was raised to increase the maximum output energy from 120 mJ to more than 150 mJ. This resulted in a slight reduction of the laser pulsewidth to  $12.2 \pm 0.5 \text{ ns}$  (FWHM). The laser beam profiles remained nearly Gaussian, as indicated by the near-field profile shown in Fig. 3. All the fibers used in the present study were from the same production lot as had been tested previously.<sup>7</sup> This lot is type FG-365-UER from 3M, having a 365- $\mu\text{m}$  diameter core of high-OH<sup>-</sup> fused silica, a 17.5- $\mu\text{m}$  thick cladding of F-doped fused silica (resulting in a numerical aperture of 0.22), a 15- $\mu\text{m}$  thick TECS<sup>TM</sup> coating, and a 150- $\mu\text{m}$  thick Tefzel<sup>®</sup> buffer. A quantity of this fiber was sent to the cleaving vendor who prepared 1-meter samples with the appropriate end faces for our testing.

At least twenty fibers having each particular type of end-face preparation were tested. The test procedure used for each fiber was similar to that used in previous studies. After alignment at very low pulse energies, a fiber was subjected to a series of single laser pulses in which the energy was increased with each successive pulse. Figure 4 shows the expected progression of measured transmitted energies assuming that no breakdown or damage occurs. The testing was halted when a breakdown or damage event did occur on a given shot. The maximum energy transmitted before this shot, together with the attempted and actual transmitted energies during this shot, were then recorded. The twenty or more measured values for highest transmitted energy before breakdown or damage were then used to generate cumulative damage probability distributions. To represent the results in this fashion, the individual fiber data were first ordered from lowest to highest transmitted energy  $E_i$  before damage, then assigned a corresponding rank  $R_i$ , where  $R_i = 1, 2, 3, \dots, N$  ( $N$  is the total number of fibers tested having a particular end-face preparation). The cumulative probability for damage  $F_i$  at energy  $E_i$  was then assigned according to:<sup>10</sup>

$$F_i = (R_i - 0.5)/N$$

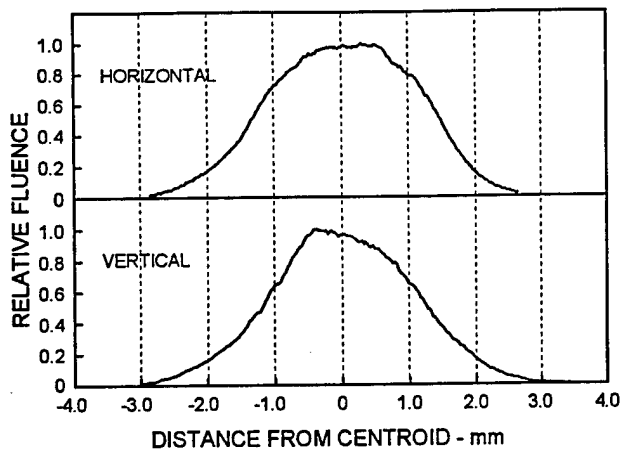


Fig. 3 Laser near-field beam profiles

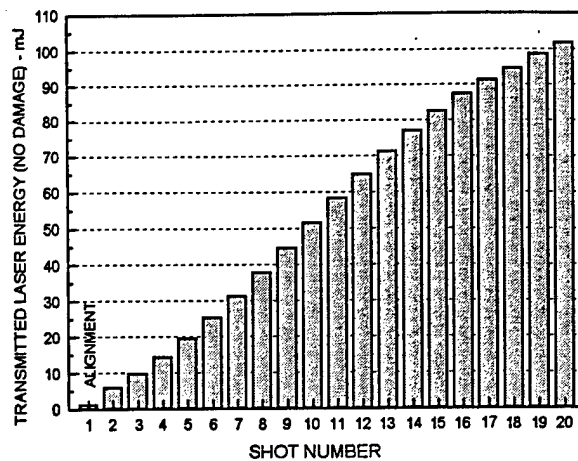


Fig. 4 Fiber test sequence

A Weibull distribution in terms of the variable  $E_i$  was obtained from a least-squares fit to the function:

$$F(E) = 1 - \exp(-E/E_0)^m$$

where  $m$  is the Weibull slope and  $E_0$  is a scale parameter. If a fiber did not damage by the end of the test sequence (Fig. 4) no value of  $E_i$  was used in the distribution fitting, but the fiber was included in the total count  $N$ . As discussed in previous studies,<sup>6,7</sup> Weibull distributions are commonly used to characterize the strength of brittle materials, in which the most serious flaw in the sample is assumed to control the strength. The most serious flaw may not be the largest, but will be where the combination of flaw size and local stress results in the largest stress intensity factor. This appears to be a good analogy to laser-induced damage in fibers, where damage thresholds will be controlled by sites where the combination of defect absorption and laser intensity is most severe. For comparison with the Weibull distributions, normal distributions were obtained from the mean and standard deviation of the  $E_i$  values. Final transmitted energies were used to calculate means and standard deviations whether fibers damaged or not. The Weibull distributions are more conservative than the normal distributions, predicting higher damage probabilities at lower energies.

Figures 5 and 6 show threshold data and probability distributions found previously during testing of mechanically polished fibers (using our best polishing schedule) and fibers which were mechanically polished and then conditioned using a  $\text{CO}_2$  laser.<sup>7</sup> This testing differed from the present study in that a simple lens injection system (50 mm focal length) and a mechanical mode scrambler were used. The results shown in these figures will be used to assess the threshold statistics generated in the present study using different end-face preparation methods.

### 3. INJECTION OPTICS

As discussed in a previous section, an ideal laser-to-fiber injection system would produce a smooth fluence distribution over most of the fiber core at the entrance face, and would quickly generate a broad mode power distribution in the fiber without any regions of internal focusing. The first goal would require some means of mitigating "hot spots" that can arise in the output from a multimode laser. An additional attribute would be insensitivity to alignment errors. An injection system based on conventional optics is not likely to achieve these features. A few years ago we began development of diffractive optical elements as components in fiber injection optics. An initial design was successful in mitigating "hot spots" and controlling the fluence distribution at the entrance face, but inadvertently produced a focused pattern at some depth into the fiber resulting in damage at low energies.<sup>5</sup> Subsequently, two more diffractive elements were designed, fabricated, and tested at Sandia National Laboratories for use in injection optics. Both of these brought improved performance, but drawbacks still precluded their use. In the past year a fourth design was developed, and several prototypes were fabricated and evaluated.<sup>11</sup> One of these prototypes was used for all the fiber damage testing in the present study.

Figure 7 is a photograph of this prototype. The diffractive element has a diameter of 6 mm, and is composed of 87 individual segments arranged within 5 concentric rings. Each segment is a low-spatial-frequency grating that diffracts

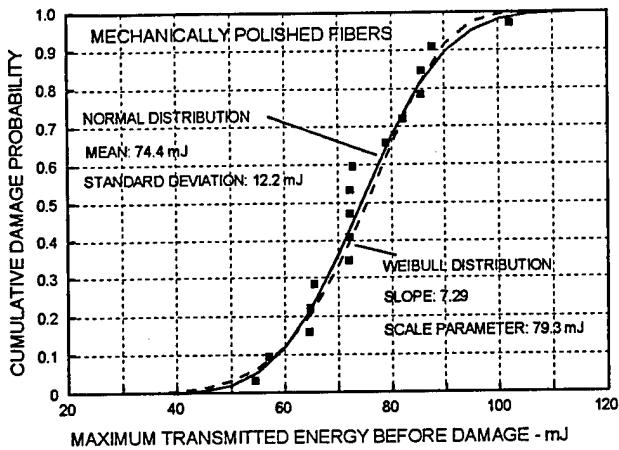


Fig. 5 Previous test results obtained with mechanically polished fibers

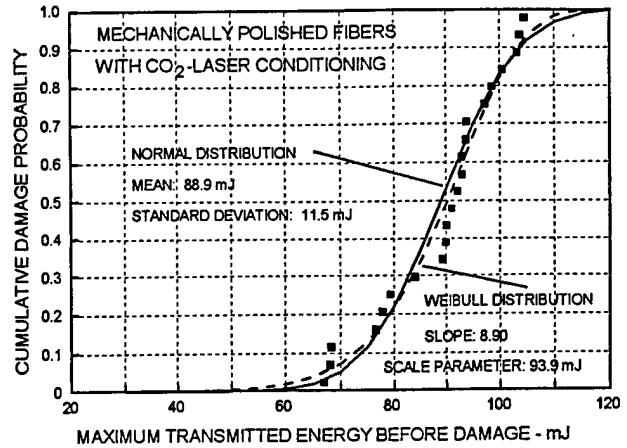


Fig. 6 Previous results obtained with mechanically polished fibers subsequently conditioned with a CO<sub>2</sub> laser

most of its incident laser light into  $\pm$  first and  $\pm$  second orders. This is achieved through a 14-level structure etched into a fused silica substrate. Design parameters were the diffraction angles and the percentage of incident light going into each order. One pair of diffraction angles was chosen for the odd-numbered rings, and a different pair of angles were used in the even-numbered rings. Within each segment the orientation of the grating is approximately radial, so the direction of the diffracted light is perpendicular (azimuthal) to this orientation. When combined with a lens, the diffractive element produces an intensity distribution in the focal plane that represents the superposition of the diffraction patterns produced by each individual segment. The distribution obtained with our test laser and a short focal length (15 mm) lens is shown in Fig. 8. The light incident upon a particular segment appears at four locations in the focal plane, with spacing that

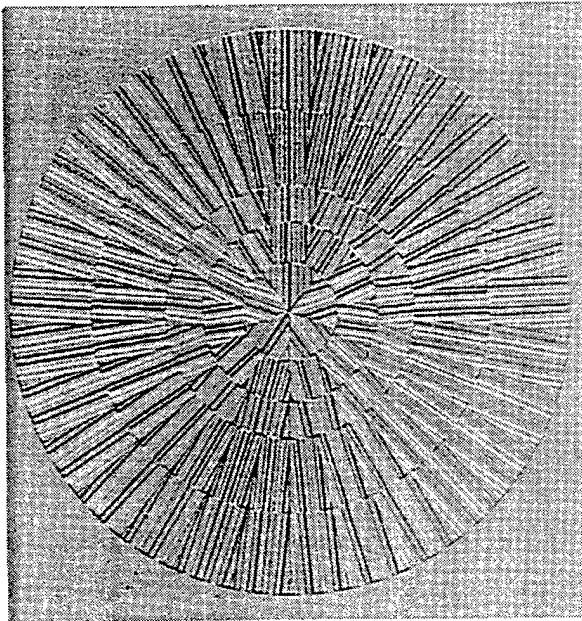


Fig. 7 The diffractive optical element used in the injection optics

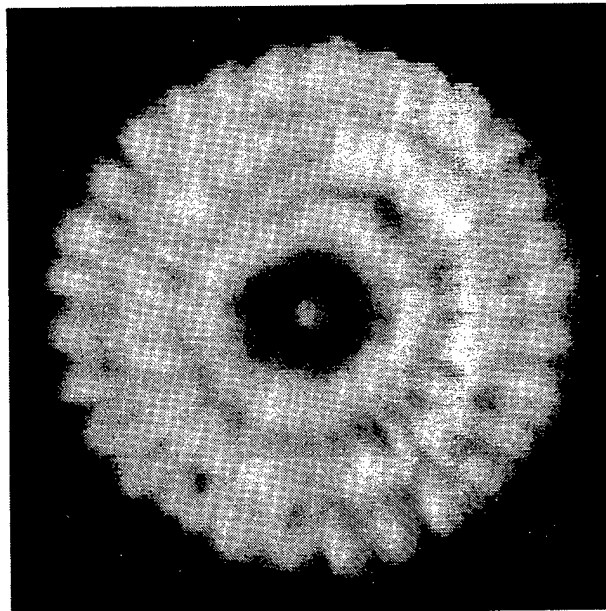


Fig. 8 The laser fluence pattern produced at the fiber entrance face

corresponds to the product of the focal length and the four diffraction angles. Because of the radial grating orientation in each segment, light approaching the focal plane has both an azimuthal component and the radial component produced by the lens. Consequently, this combination results in skew rays entering the fiber.

For given laser characteristics, the design parameters available for each diffractive segment and the arrangement of segments over the cross-sectional area of the laser beam permit considerable control over the resulting fluence distribution at a fiber entrance face positioned at the focal plane. Mitigation of "hot spots" in the beam occurs because light incident on a given segment is divided into four locations on the fiber face. The skew angles introduced by the diffractive segments prevent internal focusing on the fiber axis beyond the entrance face. The use of a lens having a very short focal length results in a broad range of entry angles within the fiber's numerical aperture, producing a broad initial mode power distribution. The use of this lens without the diffractive element would not be possible, as air breakdown at low energies would occur. Figure 9 shows beam profiles at the location of a fiber entrance face recorded using a magnified beam-profiling system. The average ratio of peak-to-average fluences measured over many individual pulses was  $P/A = 2.27$ , with a standard deviation of 0.06. This is the lowest value of this ratio that we have measured using our test laser. However, because the diffractive element successfully avoids putting light into the zero (undiffracted) order, the lowest fiber modes are relatively unpopulated. Because the typical fiber path during our testing (straight except for one 15-cm diameter,  $360^\circ$  loop) does not mix modes very effectively, the near-field laser profile at the fiber exit face has reduced fluences near the fiber centerline, as shown in Fig. 10. A more serious drawback with the diffractive element is its relative inefficiency. Losses

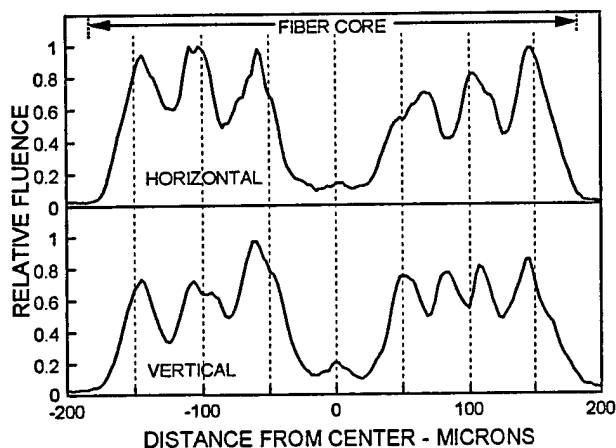


Fig. 9 Laser beam profiles at the fiber entrance face

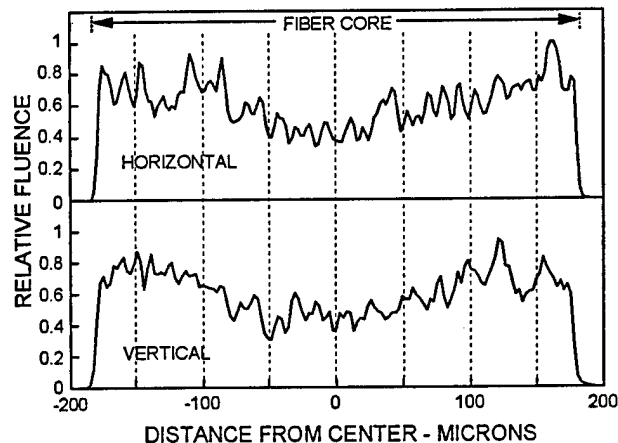


Fig. 10 Laser profiles at the exit face of a test fiber

result from diffraction into higher orders, with the corresponding light passing outside of the fiber core, and also from light scattered from the multi-level diffractive structure. We looked at a larger area of the plane containing the fiber entrance face using beam-profiling at lower magnification, and found that less than 92% of the light arriving at this plane was within the fiber core area. Overall losses were found by comparing the energy transmitted by a carefully aligned fiber with and without the diffractive element in place. These comparisons had to be made at low energies to avoid breakdown when the diffractive element was removed. With the element in place, the transmitted energy was 74.5% of the value measured with the element removed. If we account for reflection losses at the uncoated surfaces of the element, then this percentage increases to 80.0%. In order to test fibers to nearly the same maximum transmitted energies as used in previous testing (Figs. 5 and 6), the laser output energy had to be increased by 30%.

The effectiveness of this injection system in inhibiting damage within a bend in the fiber path was examined in the same manner as we had used to characterize the performance of a mechanical mode scrambler.<sup>7</sup> Figure 11 shows two horizontal beam profiles representing fiber near-field distributions at a position within a constant-radius bend. The techniques used to obtain these profiles were described in an earlier study.<sup>6</sup> The top profile shows the highly non-uniform distribution characteristic of simple lens injection. The bottom profile shows the same measurement using the current injection optics.

#### 4. RESULTS

The commercially cleaved fiber faces looked perfectly smooth, with no roughened regions and no visible edge damage corresponding to where the cleaving crack was generated. Our experience would suggest that an exceptionally good cleaving technique was used. The faces were inspected at 400 magnification using a Nomarski microscope. They had been cleaved with the 15- $\mu\text{m}$  thick TECS™ coating in place, which we removed near the face using acetone to avoid any laser energy incident on this polymer. The faces were contaminated from the shipping materials, and were cleaned using

methanol. However, we found them very difficult to completely clean as observed with our microscope. Small specks on the surface were very persistent, and small ambient particulates would often adhere to the surface within a few minutes. Figure 12 shows the results obtained with cleaved-only fibers that were carefully cleaned up to the moment that testing

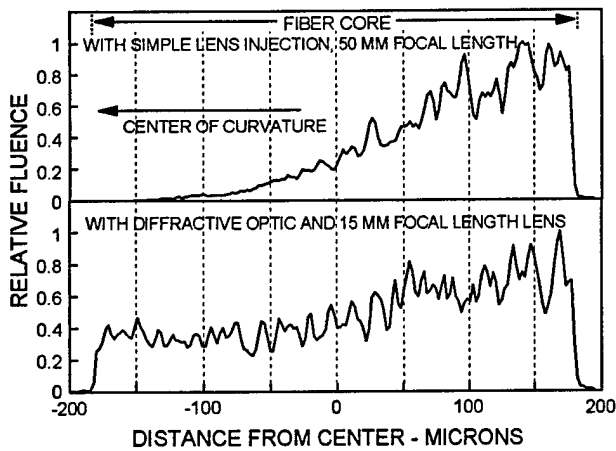


Fig. 11 Effect of current injection optics on fiber near-field profile at a position  $24^\circ$  beyond the start of a bend with a constant 7.5-cm radius

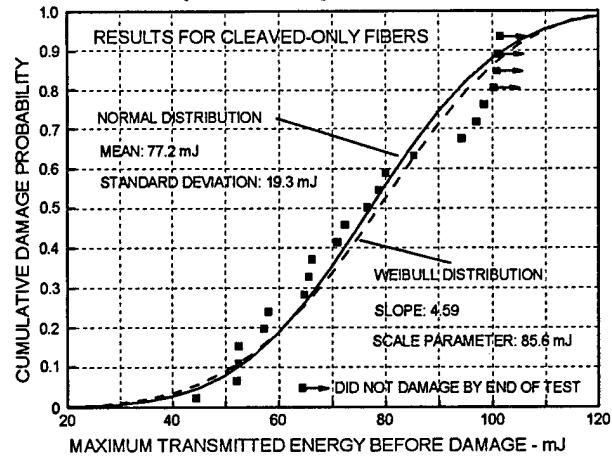


Fig. 12 Test results using cleaved-only fibers

began. The mean value of maximum transmitted energy before breakdown or damage, together with the corresponding Weibull scale parameter, are slightly higher than obtained previously with mechanically polished fibers (Fig. 5). However, the standard deviation (and the reciprocal of the Weibull slope) were substantially larger, corresponding to a much broader distribution. Sixteen of the twenty-three tested fibers experienced entrance-face breakdown, three fibers had exit-face damage, and four fibers reached the end of the test sequence.

The vendor-supplied fibers that had been flame polished following cleaving looked extremely smooth under our microscope. The edges were rounded within the cladding thickness, and the TECS™ coating was eliminated near the face. Cleaning the contamination from shipping materials using methanol was routine. Figure 13 shows the results obtained with these fibers. Contrary to our expectations, these surfaces did not show improved resistance to breakdown or damage. The mean value for maximum transmitted energy was essentially the same as with the cleaved-only fibers, and the overall distributions were even broader. Nine of the twenty tested fibers experienced entrance-face breakdown, one fiber had "entry" damage, six fibers had exit-face damage, and four fibers reached the end of the test sequence.

The experimental configuration and procedures for CO<sub>2</sub>-laser conditioning of fiber end faces was described previously.<sup>7</sup> In developing a schedule for conditioning of cleaved fibers, we found that the schedule developed for mechanically polished fibers heated the end face excessively. The final schedule developed for cleaved faces had a flatter intensity distribution with a much lower peak value. As in the previous schedule, 30-second exposures were used while the fiber face was rotated. The final surfaces were very smooth with slightly more rounding near the edge than the flame polished fibers. As in the testing of cleaved-only fibers, cleaning the cleaved surfaces prior to conditioning proved frustrating. Following the same cleaning procedures as before, we first tested half of a group of twenty fibers. These initial results were disappointing in that a broad distribution of final transmitted energies was again apparent. For the final ten fibers in this group we used a special cleaning procedure. First, a neutralizing air flow provided by a Desco bench top ionizer was added to the cleaning and conditioning area within our lab. Next, a cleaning cloth containing ultrafine fibers (CLETOP Optical Fiber Connector Cleaner, NTT International) was used to mechanically scrub the cleaved surfaces. Finally, the surfaces were cleaned conventionally with methanol. The results obtained from both parts of this group of fibers are shown in Fig. 14. The open-faced symbols in this figure represent the fibers subjected to the special cleaning procedure. Six of the second group of fibers reached the end of the test sequence, and the remaining fibers had breakdowns at relatively high energies. The distributions shown in Fig. 14 were fit to the combined testing results. Six of the total group of twenty fibers experienced entrance-face breakdown, six fibers had exit-face damage, and eight fibers reached the end of the test sequence.

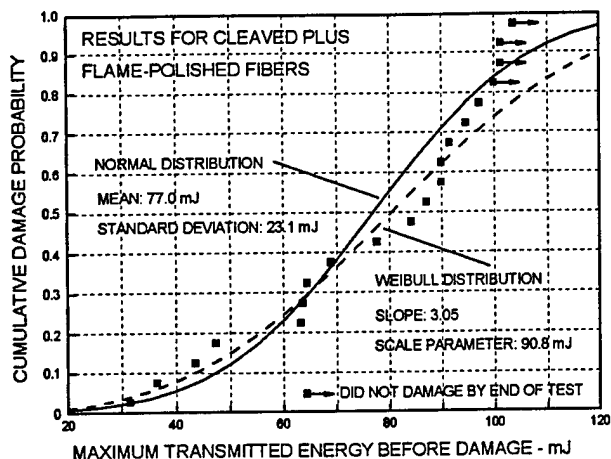


Fig. 13 Test results using cleaved fibers subsequently flame polished

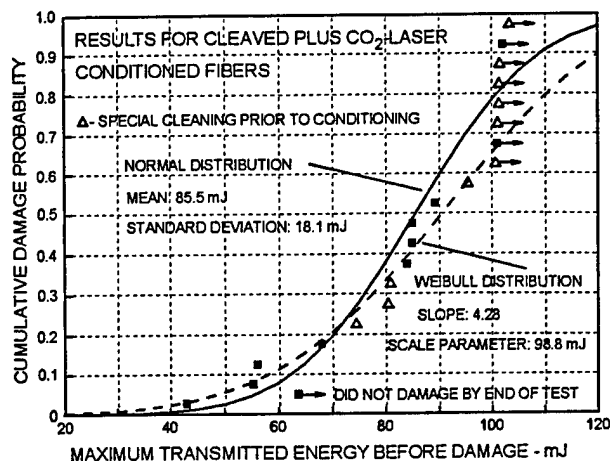


Fig. 14 Test results using cleaved fibers subsequently conditioned with a CO<sub>2</sub> laser

## 5. DISCUSSION

In the present study we evaluated three methods for fiber end-face preparation that were based on the availability of exceptionally good cleaved surfaces from a commercial vendor. These results were compared to previous measurements obtained with fibers that had been mechanically polished using an optimized polishing schedule, and with similar fibers that had subsequent conditioning using a CO<sub>2</sub> laser. The mean values for maximum transmitted energy before breakdown or damage for the cleaved-only and cleaved-plus-flame polished fibers were slightly higher than the corresponding mean value for mechanically polished fibers. The mean value for the CO<sub>2</sub>-laser conditioned fibers was somewhat higher still, but not as high as the previous result for fibers with this conditioning. More importantly, the range of maximum energy values recorded for each of the present cases was much broader than in previous studies. Consequently, probabilities for breakdown or damage at relatively low energies would be much higher. We believe that this variability in breakdown and damage thresholds is related to the difficulties we encountered in trying to clean the cleaved surfaces. A freshly cleaved surface is very active chemically, and the cleaving environment will govern the subsequent surface reactions and the final surface composition.<sup>12</sup> Despite the fact that months had passed since our fibers had been cleaved, they continued to show far more electrostatic behavior than surfaces with different or additional processing. The flame polishing performed by the vendor did not reduce the variability, indicating that features of the cleaved surfaces that were responsible for low-energy breakdowns were not being eliminated by this additional processing.

The results obtained in two parts with cleaved fibers that were subsequently conditioned with a CO<sub>2</sub> laser indicated that the variability in thresholds could be reduced. Adding a neutralizing air flow to the cleaning and processing environment, together with a mechanical "scrubbing" of the cleaved surface, clearly resulted in improved resistance to breakdown after the CO<sub>2</sub>-laser conditioning. It seems reasonable to expect that these additional steps would prove beneficial for subsequent flame polishing as well. The benefit of these additional steps on cleaved-only fibers was not investigated. The present results indicate that cleaved-only fibers are not good candidates for high-intensity applications unless some means for achieving long-term surface inertness can be found.

Three of the cleaved-only fibers, six of the fibers with flame polishing, and six of the CO<sub>2</sub>-laser conditioned fibers damaged at their exit faces. Exit-face damage is typically a consequence of subsurface defects produced by surface processing steps rather than the quality of the final surface finish. Observing this type of damage in a cleaved surface indicates that subsurface fractures are formed during the cleaving process. As is typical for this type of fiber damage mechanism,<sup>7</sup> large craters were formed in the exit faces with substantial material removal. We have observed that exit-face damage in mechanically polished fibers occurs randomly throughout the cross-sectional area of the fiber core. However, the exit-face damage observed in the present study occurred only at sites along the edge of the fiber core. Most cases had a single damage site at this edge, but a few fibers also showed some damage at the opposite edge location as well. An example of this damage morphology is shown in Fig. 15. When a fiber is cleaved, a crack is generated mechanically at one edge and propagates across the fiber cross-section under axial tension. Skillful techniques are needed to suppress crack

acceleration and instabilities before the crack reaches the opposite edge. The present results indicate that subsurface fracturing is predominant at one or both of these edges, and the subsequent processing by flame polishing or by CO<sub>2</sub>-laser conditioning did not significantly mitigate these features. Consequently, even though the cleaved surfaces appear remarkably good under our microscope, and means were found to achieve very good resistance to entrance-face breakdown with additional processing, their susceptibility to exit-face damage even after additional processing may limit the high-intensity applicability of any of the end-face processing methods examined in this study.

In the present study we also utilized an improved laser-to-fiber injection system consisting of a custom diffractive optical element and a lens with a very short focal length. This combination was successful in meeting the attributes desirable for an injection system (section 3). Most significantly, this combination was very successful in mitigating damage at internal sites along the fiber path. In the previous study with mechanically polished fibers (Fig. 5), eleven out of sixteen fibers experienced entrance-face breakdown, one fiber had exit-face damage, and four fibers damaged internally. When CO<sub>2</sub>-laser conditioning was added (Fig. 6), improved resistance to entrance-face breakdown resulted in higher laser levels passing beyond the entrance face and eventually triggering other damage mechanisms. Four out of 22 fibers experienced entrance-face breakdown, one fiber had exit-face damage, two fibers reached the end of the test sequence, and fifteen fibers damaged internally. The average energy transmitted before internal damage was 87.2 mJ. Test fibers were constrained to exactly the same path in the present study, and the basic difference in the testing configuration was that the new injection optics replaced a simple injection lens and mechanical mode scrambler. Of the 63 fibers tested in the current study, 27 of these fibers transmitted more than 87.2 mJ, and sixteen reached the end of the test sequence after transmitting more than 100 mJ. Despite the fact that a substantial number of fibers transmitted very high energies, only one fiber experienced internal ("entry") damage after transmitting 92 mJ.

The new injection system did have a few drawbacks, however, and the current design for the diffractive element could be further optimized. The laser profiles shown in Figs. 8 and 9 contain local fluences near the edge of the fiber core that are as high as local fluences closer to the fiber center. Figure 16 is a photograph of a cleaved entrance face that has experienced several damaging laser pulses. The damage pattern is consistent with the two-dimensional profile shown in Fig. 8, with

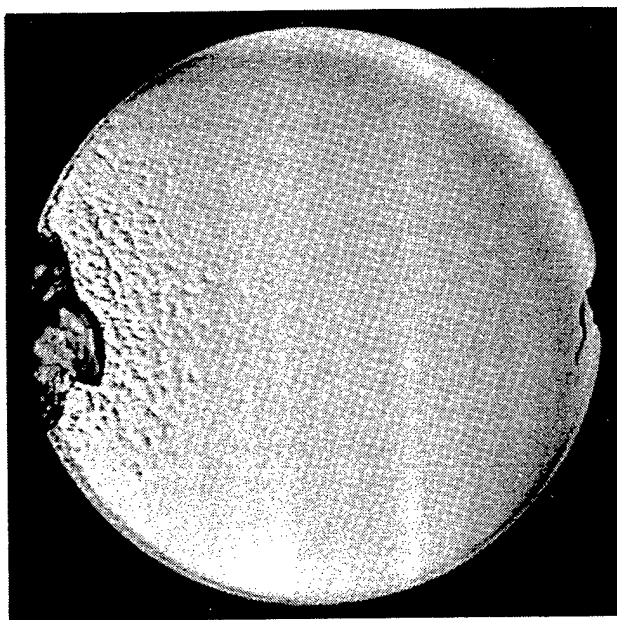


*Fig. 15 Exit face damage*

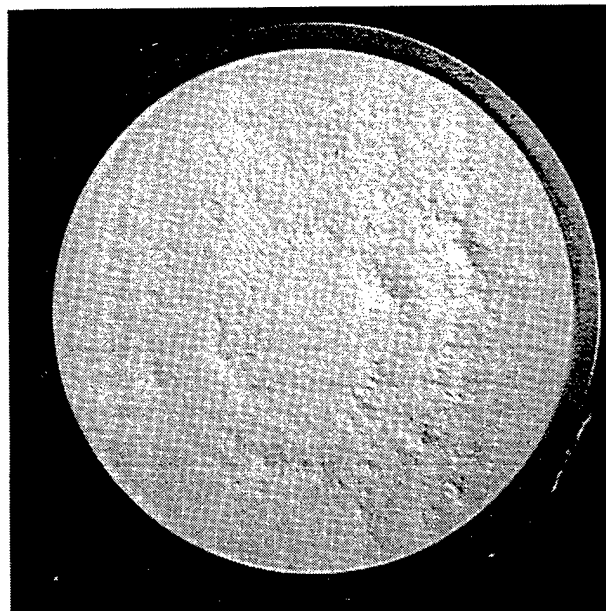


*Fig. 16 Front face damage produced by several damaging laser shots*

damage features extending close to the core/cladding interface. Although this is consistent with the objective of minimizing the ratio of peak-to-average fluences, in practice it may not be possible to achieve breakdown-resistant surface characteristics uniformly over the entire fiber core. In particular, we believe that the beneficial effects of CO<sub>2</sub>-laser conditioning are more readily obtained near the fiber center than near the core/cladding interface. Consequently, a more

optimized design would reduce the energy diffracted at the highest angle. The fact that very little energy is undiffracted prevents light from focusing along the fiber axis, but results in the lowest fiber modes being relatively unpopulated. Laser fluences at the fiber exit face were higher near the core/cladding interface than at the center (Fig. 10), and this probably contributed to the number of fibers that experienced exit-face damage at an edge. However, we found that the mode mixing introduced by adding tighter bends in the fiber path (a 5-cm diameter, 360° loop either before or after the existing 15-cm diameter loop) was sufficient to flatten the exit-face profile very effectively. Such bends are expected in our applications, and the initial lack of lower fiber modes is probably not a design issue. The most serious drawback is the fact that when the diffractive element is put into place, the energy transmitted by a fiber falls by 25%. This may be an acceptable loss in return for improved breakdown and damage thresholds, but a limited energy budget in some applications could dictate that some reduction in this loss would be needed.

## 6. ACKNOWLEDGMENTS

This work was supported by the United States Department of Energy under Contract DE-AC04-94AL85000. Sandia is a multiprogram laboratory operated by Sandia Corporation, a Lockheed Martin Company, for the United States Department of Energy. The diffractive optical element used in this study was the result of a development effort having initial contributions from Michael W. Farn, Stanford Law School (previously at Lincoln Laboratory, MIT), and sustained contributions from William C. Sweatt and Mial E. Warren, Sandia National Laboratories. The talented contributions of Dante M. Berry, Sandia National Laboratories, in CO<sub>2</sub>-laser conditioning of fibers and in performing damage testing were greatly appreciated.

## 7. REFERENCES

1. J. A. Harrington, "An Overview of Power Delivery and Laser Damage in Fibers," Proc. SPIE 2966, 536 (1997). Also: the nine following papers in Proc. SPIE 2966.
2. R. E. Setchell, K. D. Meeks, W. M. Trott, P. Klingsporn, and D. M. Berry, "High-Power Transmission Through Step-Index, Multimode Fibers," Proc. SPIE 1441, 61 (1991).
3. R. E. Setchell and P. Klingsporn, "Laser-Induced Damage Studies on Step-Index, Multimode Fibers," Proc. SPIE 1624, 56 (1992).
4. R. E. Setchell, "Laser-Induced Damage in Step-Index, Multimode Fibers," Proc. SPIE 1848, 15 (1993).
5. R. E. Setchell, "Damage Studies in High-Power Fiber Transmission Systems," Proc. SPIE 2114, 87 (1994).
6. R. E. Setchell, "Reduction in Fiber Damage Thresholds Due to Static Fatigue," Proc. SPIE 2428, 54 (1995).
7. R. E. Setchell, "An Optimized Fiber Delivery System for Q-switched, Nd:YAG Lasers," Proc. SPIE 2966, 608 (1997).
8. Pioneer Optics Company, 1000 Old County Circle, Windsor Locks, CT 06096
9. R. A. House, J. R. Bettis, A. H. Guenther, and R. Austin, "Correlation of Laser-Induced Damage with Surface Structure and Preparation of Techniques of Several Optical Glasses at 1.06  $\mu\text{m}$ ," Laser-Induced Damage in Optical Materials: 1975, National Bureau of Standards Special Publication 435, p. 305, 1976.
10. B. Bergman, "On the Estimation of the Weibull Modulus," J. Mater. Sci. Lett. 3, 689 (1984).
11. W. C. Sweatt, R. E. Setchell, M. E. Warren, and M. W. Farn, "Injecting a Pulsed YAG Laser Beam into a Fiber," Proc. SPIE 3010, 266 (1997).
12. L. Holland, The Properties of Glass Surfaces, Chapman and Hall, London, 1964, pp. 293-294.

M98003412



Report Number (14) SAND--98-0681C  
CONF-9710116--

Publ. Date (11) 199710

Sponsor Code (18) DOE/DP, XF

UC Category (19) UC-700, DOE/ER

DOE